

# A Dynamic Additive and Multiplicative Effects Network Model with Application to the United Nations Voting Behaviors

Bomin Kim<sup>1</sup>, Xiaoyue Niu<sup>2</sup>, David Hunter<sup>2</sup>, and Xun Cao<sup>3</sup>

<sup>1</sup>Freddie Mac

<sup>2</sup>Department of Statistics, The Pennsylvania State University

<sup>3</sup>Department of Political Science, The Pennsylvania State University

## Abstract

We introduce a regression model for a series of networks that are correlated over time. Our model is a dynamic extension of the additive and multiplicative effects network model (AMEN) of Hoff (2019). In addition to incorporating a temporal structure, the model accommodates two types of missing data thus allows the size of the network to vary over time. We demonstrate via simulations the necessity of various components of the model. We apply the model to the United Nations General Assembly voting data from 1983 to 2014 (Voeten (2013)) to answer interesting research questions regarding to international voting behaviors. In addition to finding important factors that could explain the voting behaviors, the model-estimated additive effects, multiplicative effects, and their movements reveal meaningful foreign policy positions and alliances of various countries.

## 1 Introduction

Network analysis is widely used in a variety of applications. There has been a lot of work in developing models for static networks. The exponential family random graph model (ERGM) (Frank and Strauss (1986)) describes the global features of a network, while the latent variable models study the both the global and local characteristics and tie formations of networks. Examples of the latent variable models include but not limited to the Stochastic Blockmodel (Snijders and Nowicki (1997) and Nowicki and Snijders (2001)) and its variants (Airoldi et al. (2008) and Karrer and Newman (2011)), and the latent space model and its variants, i.e. the distance and projection models, (Hoff et al. (2002)), the bilinear effects model (Hoff (2005)), and the additive and multiplicative effects model (AME) (Hoff (2019)).

Networks naturally evolve over time. With the availability of more data, there has been a growing need for modeling a series of networks that change over time. New models have been proposed to depict the network evolution, such as the stochastic actor oriented models in Snijders (2001), Snijders et al. (2007) and Snijders et al. (2010). Others have extended static network models mentioned above to the dynamic case. For example, Robins and Pattison (2001), Hanneke et al. (2010), and Krivitsky and Handcock (2014) are dynamic versions of ERGM. Various literature has proposed dynamic stochastic blockmodels (Xing et al., 2010; Ho et al., 2011; Yang et al., 2011; Xu and Hero, 2013; Matias and Miele, 2017). Different versions of the dynamic latent space model ((Sarkar and Moore, 2006; Sarkar et al., 2007; Sewell and Chen, 2015, 2016; Friel et al., 2016)) extend the latent distance model, and Durante and Dunson (2014) extend a simplified version of the bilinear effects model. For a more comprehensive review of the literature on dynamic network models with latent variables, see Kim et al. (2018).

In this article, we would like to focus on the AME framework. Specifically, the Gaussian additive and multiplicative effects model for asymmetric relational data assumes

$$Y_{ij} = \sum_{p=1}^P X_{ijp} \beta_p + a_i + b_j + \mathbf{u}'_i \mathbf{v}_j + \epsilon_{ij}, \quad (1)$$

where  $Y_{ij}$  is the  $(ij)$ th entry of the sociomatrix ( $\mathbf{Y}_{n \times n}$ ) of the network;  $\boldsymbol{\beta} = (\beta_1, \dots, \beta_P)$  is the  $P$ -length coefficient vector of predictor ( $\mathbf{X}_{n \times n \times P}$ ) effects (including the intercept);  $a_i$  and  $b_j$  are the row and column additive effects, which can be interpreted as node  $i$ 's "sociability" and node  $j$ 's "popularity";  $\mathbf{u}_i$  and  $\mathbf{v}_j$  are the latent factors of rank  $R$ ; and the multiplicative effects of  $\mathbf{u}_i' \mathbf{v}_j$  represent the similarity between node  $i$  and node  $j$ . To give more interpretation of the latent factors, if  $\mathbf{u}_i \approx \mathbf{v}_j$ , they are close in the latent space. Node  $i$  and  $j$  will generate a large response in a valued network and be more likely to form a tie in a binary network. If  $\mathbf{u}_i \approx \mathbf{u}_j$ , node  $i$  and node  $j$  are considered playing a similar role in the network that they are stochastic equivalent.

For symmetric relational data, the AME model can be expressed as the following:

$$Y_{ij} = \sum_{p=1}^P X_{ijp} \beta_p + a_i + a_j + \mathbf{u}_i' \mathbf{D} \mathbf{u}_j + \epsilon_{ij}, \quad (2)$$

where rather than the symmetric version of the bilinear term  $\mathbf{u}_i' \mathbf{u}_j$ , we use this more general form of eigenvalue decomposition and include the diagonal matrix  $\mathbf{D} = \text{diag}(\mathbf{D}_1, \dots, \mathbf{D}_R)$  to allow for positive and negative values that can represent both homophily and anti-homophily. In addition to the interpretation in the asymmetric case, if  $\mathbf{u}_i \approx \mathbf{u}_j$ , that is they are very close in the latent space, with a positive  $\mathbf{D}_r$ , they will produce a large response in a valued network and be more likely to form a tie in a binary network. This would correspond to homophily. On the other hand, with negative  $\mathbf{D}_r$ , node  $i$  and  $j$  will produce a small response and be less likely to form a tie. This would correspond to anti-homophily.

Under the AME framework, all of the model parameters have clear interpretation and capture various features of the network. The fixed effects explain the global feature and observed covariate (nodal and dyadic) effects of the network. The additive effects describe the across-row and across-column heterogeneities, which are second order dependence measured by covariances. The multiplicative factors capture the non-additive, higher order dependence that generates homophily, transitivity, balance, and stochastic equivalence. Hoff (2008) shows that the latent factor representation is a general class that contains the latent distance model and the stochastic blockmodel. To the best of our knowledge, the AME model has not been extended to the dynamic case, and that is our focus in this article.

Most of the dynamic extensions from the static models pose a Markov assumption on the time dependence, i.e. the current state only depends on the one from the most recent time point. This assumption eliminates the possibility of long memory processes and implicitly relies on equal spacing between time points in the data. One exception is Durante and Dunson (2014), which extends a simplified version of the symmetric bilinear effects model, that is a model with the term  $\mathbf{u}_i' \mathbf{u}_j$ . It assumes a Gaussian process prior on the  $\mathbf{u}(t)$ . The Gaussian process would allow one to model the dependence between any two time points through a covariance function. Durante and Dunson (2014) picks the squared exponential covariance function and predetermines the length scale parameter in the covariance structure. Without prior knowledge of the data, fixing the covariance structure limits the flexibility and generalizability of the model.

Another challenge in dynamic network modeling is missing data, including missing edges and missing nodes over time. Common practice is either using the subset of nodes that have complete observations, or treating all of the missing data as missing at random and imputing them. We argue that some of the missing mechanisms might not be missing at random, especially the missing nodes over time. We would like to make distinct treatments for different missing mechanisms.

In summary, our goal for this article is to combine the advantage of the AME framework and the Gaussian process dependence structure and propose a dynamic additive and multiplicative effects (DAME) network model. We will allow different forms of the covariance structure in the Gaussian process and estimate the length scale from the data. The proposed model will also allow various types of missing data.

In Section 2, we introduce the DAME model, derive the sampling distribution for Bayesian inference, and describe the treatment of missing data. Then we present simulation studies to show the necessity of various components in the DAME model. And in Section 4 we apply the DAME model to the United Nations General Assembly voting network, demonstrate the validity of the model and discuss the findings.

## 2 Dynamic Additive and Multiplicative Effects Model

### 2.1 Model Formulation

Our main goal is to build a regression model for the sequence of  $N \times N$  time-varying matrices  $\mathbf{Y} = \{\mathbf{Y}^1, \dots, \mathbf{Y}^T\}$ , where the entry  $y_{ij}^t$  denotes the relational data corresponding to the node pair  $(i, j)$  at timepoint  $t$ ,  $t = 1, 2, \dots, T$ . The observed covariate arrays are denoted by  $\mathbf{X} = \{\mathbf{X}^1, \dots, \mathbf{X}^T\}$ , where  $\mathbf{X}^t = \{\mathbf{X}_1^t, \dots, \mathbf{X}_P^t\}$ . Here we focus on extending the AME model for symmetric relations in (2). The asymmetric version can be extended in a similar fashion which is discussed in the last section. For  $i = 2, \dots, N, j = 1, \dots, i - 1$ , and  $t = 1, \dots, T$ , we assume

$$y_{ij}^t = \sum_{p=1}^P X_{ijp}^t \beta_p^t + a_i^t + a_j^t + \mathbf{u}_i^{t'} \mathbf{D}^t \mathbf{u}_j^t + \epsilon_{ij}^t, \quad (3)$$

where  $X_{ijp}^t$  is the  $p$ th covariate,  $\beta_p^t$  is the corresponding unknown coefficient,  $a_i^t$  and  $a_j^t$  are the node-specific additive random effects,  $\mathbf{u}_i^t = [u_{i1}^t, \dots, u_{iR}^t]'$  denotes the  $R$ -length latent vector of node  $i$ ,  $\mathbf{D}^t$  is an  $R \times R$  diagonal matrix with diagonal entries  $d_{11}^t, \dots, d_{RR}^t$ , and  $\epsilon_{ij}^t$  is the random error.

To model the temporal dependence in the networks, we assume Gaussian process (GP) priors for the parameters  $\boldsymbol{\beta}$ ,  $\mathbf{a}$  and  $\mathbf{u}$ :

1. For  $p = 1, \dots, P$ ,

$$\begin{aligned} \boldsymbol{\beta}_p &\sim \mathcal{N}_T(\mathbf{0}, \Sigma_p^\beta), \\ \Sigma_p^\beta &= \tau_p^\beta f(\kappa_p^\beta), \end{aligned}$$

where  $\boldsymbol{\beta}_p = (\beta_p^1, \dots, \beta_p^T)$  is a  $T$ -dimensional vector and  $\Sigma_p^\beta$  is a  $T \times T$  covariance matrix with variance parameter  $\tau_p^\beta$  and range parameter  $\kappa_p^\beta$ .

2. For  $i = 1, \dots, N$ ,

$$\begin{aligned} \mathbf{a}_i &\sim \mathcal{N}_T(\mathbf{0}, \Sigma^a) \\ \Sigma^a &= \tau^a f(\kappa^a), \end{aligned}$$

where  $\mathbf{a}_i = (a_i^1, \dots, a_i^T)$  is a  $T$ -dimensional vector and  $\Sigma^a$  is a  $T \times T$  covariance matrix with variance parameter  $\tau^a$  and range parameter  $\kappa^a$ .

3. For  $i = 1, \dots, N$  and  $r = 1, \dots, R$ ,

$$\begin{aligned} \mathbf{u}_{ir} &\sim \mathcal{N}_T(\mathbf{0}, \Sigma_r^u), \\ \Sigma_r^u &= \tau_r^u f(\kappa_r^u), \end{aligned}$$

where  $\mathbf{u}_{ir} = (u_{ir}^1, \dots, u_{ir}^T)$  is a  $T$ -dimensional vector and  $\Sigma_r^u$  is a  $T \times T$  covariance matrix with variance parameter  $\tau_r^u$  and range parameter  $\kappa_r^u$ .

The key part of the Gaussian process is the formulation of covariance matrices  $\Sigma_1^\beta, \dots, \Sigma_P^\beta, \Sigma^a$ , and  $\Sigma_1^u, \dots, \Sigma_R^u$ . We consider two of the commonly used covariance functions (Rasmussen, 2003), the standard exponential (or Ornstein–Uhlenbeck) function and the squared exponential function. The standard exponential function has the following form:

$$f_{tt'}(\kappa) = \exp\left(-\frac{|t - t'|}{\kappa}\right),$$

where  $|t - t'|$  is the absolute distance between the two time points  $t$  and  $t'$ . If we replace the distance term by  $|t - t'|^2$  it becomes the squared exponential function. For discrete dynamic process when the time intervals are reasonably spaced, we would prefer the standard exponential function. On the other hand, if the time interval is very small or we are modeling a continuous process where smoothness is expected, the squared form is preferred. Durante and Dunson (2014) fix the parameter  $\kappa$  that characterizes the length-scale of the process. In practice, prior knowledge on how much the networks are correlated over time is usually unavailable. Different choices of  $\kappa$  would lead to different outcomes in model performance. To avoid the challenge of choosing an appropriate value of  $\kappa$ , we jointly estimate  $\tau$  and  $\kappa$  assuming inverse-Gamma and half-Cauchy priors, respectively, that is:

$$\begin{aligned}
\tau_p^\beta &\sim \mathcal{IG}(k_\beta, \theta_\beta) \text{ and } \kappa_p^\beta \sim \text{half-Cauchy}(\gamma_\beta) \text{ for } p = 1, \dots, P, \\
\tau^a &\sim \mathcal{IG}(k_a, \theta_a) \text{ and } \kappa^a \sim \text{half-Cauchy}(\gamma_a), \\
\tau_r^u &\sim \mathcal{IG}(k_u, \theta_u) \text{ and } \kappa_r^u \sim \text{half-Cauchy}(\gamma_u) \text{ for } r = 1, \dots, R.
\end{aligned}$$

4. We assume independent normal prior for the diagonal matrix  $\mathbf{D}$  rather than another Gaussian process for identifiability reasons. For  $r = 1, \dots, R$  and  $t = 1, \dots, T$ ,

$$d_r^t \sim \mathcal{N}(\mathbf{0}, I_R),$$

where  $I_R$  is the  $R \times R$  identity matrix.

5. Finally, we assume normal error terms with inverse-Gamma priors for the variance parameter. For  $i = 1, \dots, N; j = 1, \dots, N$ , and  $t = 1, \dots, T$ ,

$$\epsilon_{ij}^t \sim \mathcal{N}(0, \sigma_e^2),$$

where  $\sigma_e^2 \sim \mathcal{IG}(k_\sigma, \theta_\sigma)$ , and the  $\epsilon_{ij}^t$  are independent given  $\sigma_e^2$ .

## 2.2 Posterior Computation

We take a Bayesian approach to infer the parameters in the DAME model. Our posterior computation is performed via a Gibbs sampler to update the vector of time-varying regression coefficients and the vector of additive and multiplicative latent factors, along with the use of the Metropolis-Hastings (MH) algorithm to sample the variance and length GP parameters  $(\tau, \kappa)$ , which is further demonstrated in Appendix B. This section outlines the steps and sampling equations for Markov Chain Monte Carlo (MCMC) updates of the DAME model, where the derivations of each step can be found in Appendix A.

To begin with, let  $\mathbf{E}^t$  denote the  $N \times N$  matrix of random noise, where the  $(i, j)^{th}$  entry is defined as

$$E_{ij}^t = y_{ij}^t - \left( \sum_{p=1}^P X_{ijp}^t \beta_p^t + a_i^t + a_j^t + \mathbf{u}_i^{t'} \mathbf{D}^t \mathbf{u}_j^t \right).$$

Given that the distribution of the observed network  $\mathbf{Y} = \{\mathbf{Y}^1, \dots, \mathbf{Y}^T\}$  conditional on all the parameters can be written as the product of Normal probability density functions (pdf)

$$\begin{aligned}
&\Pr(\mathbf{Y} | \mathbf{X}, \boldsymbol{\beta}, \mathbf{a}, \mathbf{d}, \mathbf{u}, \sigma_e^2, \boldsymbol{\tau}^\beta, \tau^a, \boldsymbol{\tau}^d, \boldsymbol{\tau}^u, \boldsymbol{\kappa}^\beta, \kappa^a, \boldsymbol{\kappa}^u) \\
&\propto \prod_{t=1}^T \prod_{i>j} (\sigma_e^2)^{-\frac{1}{2}} \exp\left\{ -\frac{1}{2\sigma_e^2} \|E_{ij}^t\|^2 \right\}, \tag{4}
\end{aligned}$$

we sequentially update each parameter from its full conditional distribution in the following sampling steps:

1. Sample  $\sigma_e^2 \sim \mathcal{IG}\left(\frac{T \cdot N(N-1)}{4} + k_\sigma, \frac{1}{2} \sum_{t=1}^T \sum_{i>j} (E_{ij}^t)^2 + \theta_\sigma\right)$ ;
2. For each  $p = 1, \dots, P$  in a random order, sample  $\boldsymbol{\beta}_p$  as follows:
  - (a) Sample  $(\tau_p^\beta, \kappa_p^\beta)$  using the MH algorithm
  - (b) Sample  $\boldsymbol{\beta}_p \sim \mathcal{N}_T(\tilde{\boldsymbol{\mu}}_{\beta_p}, \tilde{\boldsymbol{\Sigma}}_{\beta_p})$  with

$$\tilde{\boldsymbol{\Sigma}}_{\beta_p} = \left( (\boldsymbol{\Sigma}_p^\beta)^{-1} + \frac{\text{diag}(\{\sum_{i>j} X_{ijp}^{t2}\}_{t=1}^T)}{\sigma_e^2} \right)^{-1} \text{ and } \tilde{\boldsymbol{\mu}}_{\beta_p} = \left( \frac{\{\sum_{i>j} (E_{ij[-p]}^t X_{ijp}^t)\}_{t=1}^T}{\sigma_e^2} \right) \tilde{\boldsymbol{\Sigma}}_{\beta_p},$$

where  $E_{ij[-p]}^t = E_{ij}^t + \beta_p^t X_{ijp}^t$  and  $\boldsymbol{\Sigma}_p^\beta = \tau_p^\beta f(\kappa_p^\beta)$ .

3. For each  $i = 1, \dots, N$  in a random order, sample  $\mathbf{a}_i$  as follows:

- (a) Sample  $(\tau^a, \kappa^a)$  using the MH algorithm
- (b) Sample  $\mathbf{a}_i \sim \mathcal{N}_T(\tilde{\mu}_{a_i}, \tilde{\Sigma}_{a_i})$  with

$$\tilde{\Sigma}_{a_i} = \left( (\Sigma_a)^{-1} + \frac{(N-1)I_T}{\sigma_e^2} \right)^{-1} \text{ and } \tilde{\mu}_{a_i} = \left( \frac{\{\sum_{j \neq i} E_{ij[-i]}^t\}_{t=1}^T}{\sigma_e^2} \right) \tilde{\Sigma}_{a_i},$$

where  $E_{ij[-i]}^t = E_{ij}^t + a_i^t$ ,  $\Sigma^a = \tau^a f(\kappa^a)$ .

4. For each  $i = 1, \dots, N$  and  $r = 1, \dots, R$  in a random order, sample  $\mathbf{u}_{ir}$  as follows:

- (a) For each  $r = 1, \dots, R$ , sample  $(\tau_r^u, \kappa_r^u)$  using the MH algorithm
- (b) Sample  $\mathbf{u}_{ir} \sim \mathcal{N}_T(\tilde{\mu}_{u_{ir}}, \tilde{\Sigma}_{u_{ir}})$  with

$$\tilde{\Sigma}_{u_{ir}} = \left( (\Sigma_r^u)^{-1} + \frac{\text{diag}(\{\sum_{j \neq i} (d_r^t u_{jr}^t)^2\}_{t=1}^T)}{2\sigma_e^2} \right)^{-1} \text{ and } \tilde{\mu}_{u_{ir}} = \left( \frac{\{\sum_{j \neq i} (E_{ij[-r]}^t d_r^t u_{jr}^t)\}_{t=1}^T}{2\sigma_e^2} \right) \tilde{\Sigma}_{u_{ir}},$$

where  $E_{ij[-r]}^t = E_{ij}^t + u_{ir}^t d_r^t u_{jr}^t$  and  $\Sigma_r^u = \tau_r^u f(\kappa_r^u)$ .

5. For each  $r = 1, \dots, R$  in a random order, sample  $\mathbf{d}_r$  as follows:

- (a) Sample  $\mathbf{d}_r \sim \mathcal{N}_T(\tilde{\mu}_{d_r}, \tilde{\Sigma}_{d_r})$  with

$$\tilde{\Sigma}_{d_r} = \left( I_T + \frac{\text{diag}(\{\sum_{i > j} (u_{ir}^t u_{jr}^t)^2\}_{t=1}^T)}{\sigma_e^2} \right)^{-1} \text{ and } \tilde{\mu}_{d_r} = \left( \frac{\{\sum_{i > j} (E_{ij[-r]}^t u_{ir}^t u_{jr}^t)\}_{t=1}^T}{\sigma_e^2} \right) \tilde{\Sigma}_{d_r},$$

where  $E_{ij[-r]}^t = E_{ij}^t + u_{ir}^t d_r^t u_{jr}^t$ .

Note that after steps 2 through 5,  $\mathbf{E} = \{\mathbf{E}^1, \dots, \mathbf{E}^T\}$  has to be calculated again using the previously updated values, so that any update is conditioned on the current values of all the other parameters.

### 2.3 Handling Missing Data

In dynamic networks, nodes or edges can be missing at any time point. If some of the edges are missing at some time point without a particular reason, we might be able to assume missing at random. However, if some nodes did not exist before a certain time point and joined later in the process, they might be missing for a particular reason and are not at random. Treating all of the edges associated with that node as missing at random might be problematic. If we decide to ignore all of the missing data and only use the complete data, we may end up with a small number of nodes losing a large amount of information. If we impute them in the same fashion, we might generate biases from those missing not at random ones. Moreover, if we have covariates in the data, the distribution of the covariates associated with the missing nodes and their relationship with the response might be different from the observed ones, which would lead to another source of bias. Therefore, we would like to treat the two missing mechanisms separately thus allow a varying number of nodes over time.

We define two types of missing data—"random missing" and "structural missing". Let the  $N \times T$  matrix  $\mathbf{A}$  denote the availability of all of the nodes  $n = 1, \dots, N$  at time  $t = 1, \dots, T$ , i.e.,

$$A_{nt} = \begin{cases} 1, & \text{node } n \text{ is available at time } t \\ 0, & \text{node } n \text{ is not available at time } t, \end{cases}$$

where  $N$  is the number of nodes who are part of the network at any time  $1 \leq t \leq T$ . Without prior knowledge on the missing mechanism, we assume that missing edges corresponding to node  $n$  at time  $t$  for which  $A_{nt} = 1$  are random missing, while those for which  $A_{nt} = 0$  are structural missing.  $\mathbf{A}$  is a known matrix once the data are given. If additional information regarding the missing mechanism is available, we can reflect it in the  $\mathbf{A}$  matrix. Random missing edges are imputed from the current estimates of parameter values at each MCMC iteration. Edges that are structural missing are excluded from the likelihood so the parameters are estimated without them. This procedure would also prevent incorrect inference by using the covariates associated with structural missing

values, where the distribution of covariates for the missing outcomes could possibly differ greatly from those for the observed outcomes. Even if the model does not contain covariates, identifying the structural missing could still be important because the imputed value could possibly overestimate or underestimate the temporal correlations of additive and/or multiplicative effects, introducing further biases.

### 3 Simulation Study

We provide a simulation study to evaluate our proposed model’s ability to capture some important properties of the data. There are two objectives in this simulation study: 1) show that estimation of the correct covariance structure plays a key role in the model performance, particularly in the case of modeling a network that is highly correlated across time, and 2) demonstrate that the eigen-decomposition formulation of the multiplicative random effects ( $\mathbf{u}'\mathbf{D}\mathbf{u}$ ) has the benefit of revealing various types of transitivity effects.

#### 3.1 Estimating Temporal Correlations

For this simulation study, we simulate three dynamic network data according to the generative process in Section 2.1, with  $N = 20$  and  $T = 10$ ,  $P = 1, R = 2$ ,  $(a, b) = (2, 1)$ , and with high ( $\kappa = 30$ ), medium ( $\kappa = 2$ ), and low correlation ( $\kappa = 0.001$ ), respectively. For each generated dataset, we fit the DAME model with 1) estimating  $\kappa$ , and 2) fixing  $\kappa$  at a wrong value. In all three cases, we run 12,000 MCMC iterations which appear to be long enough for full convergence, and then discard the first 2,000 samples with a thinning interval of 20.

To summarize our simulation results, we define a “lag-1 degree correlation” by calculating the Pearson correlation  $\rho(\cdot)$  between the vectors  $v_1$  and  $v_2$ , with:

$$\begin{aligned} v_1 &= [\text{degrees}(\mathbf{Y}^1), \dots, \text{degrees}(\mathbf{Y}^{T-1})], \\ v_2 &= [\text{degrees}(\mathbf{Y}^2), \dots, \text{degrees}(\mathbf{Y}^T)], \end{aligned} \tag{5}$$

where  $\text{degrees}(\mathbf{Y}^t)$  indicates the vector of degree statistics for all nodes, so that  $v_1$  and  $v_2$  both have length  $N \times (T - 1)$ . More specifically,  $\text{degrees}(\mathbf{Y}^t) = (\sum_{j=1}^N y_{1j}^t, \sum_{j=1}^N y_{2j}^t, \dots, \sum_{j=1}^N y_{Nj}^t)$ . At each iteration of the MCMC, we generate a posterior predicted  $\mathbf{Y}$  and calculate the lag-1 degree correlation.

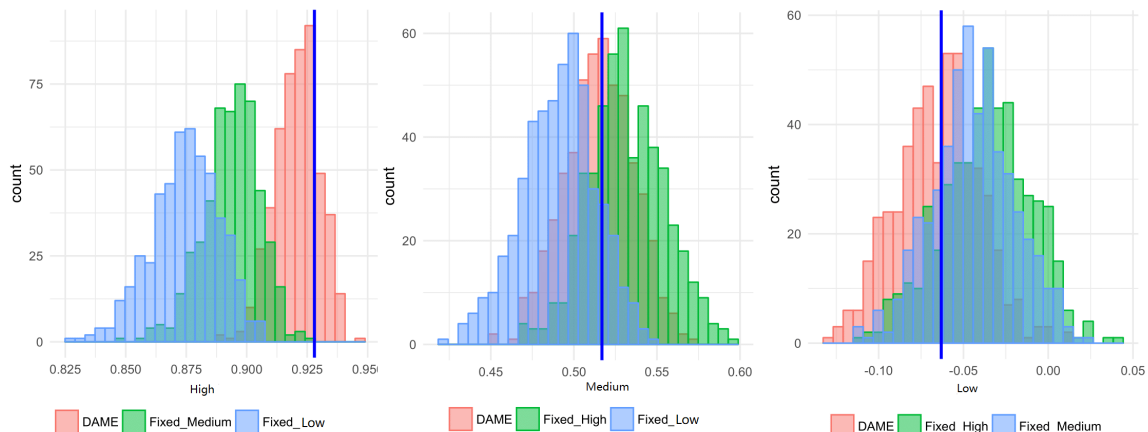


Figure 1: Histogram of posterior distributions of the lag-1 degree correlations. The temporal correlations of the networks are high (*left*), medium (*middle*), and low (*right*). The vertical line in each plot represents the true value of the lag-1 degree correlation.

Figure 1 compares the posterior distribution of lag-1 degree correlations from DAME model and the “fixed models” under the three scenarios. For the high correlation case (*left*),  $\kappa$  is fixed at 2

and 0.001 to represent mis-specifying at medium and low values. For the medium correlation case (middle),  $\kappa$  is fixed at 30 and 0.001 to represent mis-specifying at high and low values. For the low correlation case (right),  $\kappa$  is fixed at 30 and 2 to represent mis-specifying at high and medium values. The true correlation is represented by the vertical line in each plot. We can see from the plots that posterior distributions of the lag-1 degree correlation from those incorrect  $\kappa$ 's all center around wrong values, while the DAME model can correctly recover this correlation. The results indicate that mis-specifying the  $\kappa$  parameter leads to biased estimation of some aspects of the network, in this case, the lag-1 degree correlation. Therefore, without prior knowledge about the temporal correlation of the network, it is necessary to treat  $\kappa$  as an unknown parameter and estimate it.

### 3.2 Estimating Homophily and Transitivity

As introduced in Section 1, the inclusion of the  $\mathbf{D}$  term in the multiplicative effects will help capture both homophily and anti-homophily. These two types of homophily effects would generate positive and negative transitivity. We test this claim by conducting another simulation study. Similar to Section 3.1, we generate  $\mathbf{Y}$  from Normal distribution with  $N = 20$ ,  $T = 10$ ,  $P = 1$ ,  $R = 2$ , and  $(a, b) = (2, 1)$ . We fix  $d_r^t = \pm 2$  for  $r = 1, \dots, R$  and  $t = 1, \dots, T$  so that the generated network exhibits 1) positive ( $d_r^t = +2$  for all  $r$  and  $t$ ), 2) mixed ( $d_1^t = -2$  and  $d_2^t = +2$  for all  $t$ ), or 3) negative ( $d_r^t = -2$  for all  $r$  and  $t$ ) transitive features, respectively. We fit the DAME model as well as the model with the bilinear effects  $\mathbf{u}'\mathbf{u}$ . We run 6,000 MCMC iterations and discard the first 1,000 with a thinning interval of 10. We fix the range parameter  $\kappa$ 's at their true values (i.e.,  $(\kappa^\beta, \kappa^a, \kappa^d) = (0, 0, 0)$ ) and do not estimate the covariance parameters. Instead, we fit the fixed models in which all parameters and the resulting dynamic networks are independent across any timepoint such that the difference in model performance only originates from the multiplicative effects formulations,  $\mathbf{u}'\mathbf{D}\mathbf{u}$  and  $\mathbf{u}'\mathbf{u}$ .

Figure 2 illustrates a graphical comparison between the two formulations of the multiplicative random effects with respect to some degree-based statistics. We first use  $\text{degree}(\mathbf{Y}^t)$ , which is defined in Section 3.1 and call this as the first moment degree. Additionally, we define the second and third moments degree statistics, denoted by  $\text{degree}(\mathbf{Y}^{t^2})$  and  $\text{degree}(\mathbf{Y}^{t^3})$ , by taking the row sums of squared matrix  $\mathbf{Y}^{t^2}$  and cubed matrix  $\mathbf{Y}^{t^3}$ , respectively. For simplicity, we only present the results from a randomly chosen node and show the posterior distribution of the three degree statistics ( $y$ -axis) over time ( $x$ -axis). For the case of positive transitivity, the two models are equivalent. As expected, they do not show any differences. In the case of mixed or negative transitivity, the two formulations reveal noticeable differences. While the DAME model can still recover the true degrees of the first to third moments, the alternative model without  $\mathbf{D}$  term shows inaccuracy in generating networks that are close to the true data in terms of the degree statistics. Not only does the alternative  $\mathbf{u}'\mathbf{u}$  model introduce bias, but also it yields significantly wider interval estimates, implying lower precision compared to the DAME model. In addition, the evidence of the  $\mathbf{u}'\mathbf{u}$  model's failure to capture the transitivity effects becomes larger as the network tends toward stronger negative transitivity and also as we move to the degree statistics in higher moments. These findings strongly support our choice of the  $\mathbf{u}'\mathbf{D}\mathbf{u}$  formulation over  $\mathbf{u}'\mathbf{u}$  to gain flexibility in modeling various types of transitivity.

## 4 Analysis of the United Nations Voting Network

### 4.1 Data Description

Votes in the United Nations General Assembly (UNGA) have been analyzed in many political science papers (Voeten, 2000, 2004; Bearce and Bondanella, 2007; Mattes et al., 2015; Bailey et al., 2017) and have become the standard data sources to study states' preferences, one of the most important topics in the field of international relations (Wendt, 1994). With regard to policy implications, for instance, states are the key actors on the global stage. Knowing their preferences towards each other and their stances on different issues helps us predict future foreign policies and state behaviors. Unfortunately, many existing studies ignore three important features of the dataset. First, votes are highly correlated over time, because they are the reflections of history. Bailey et al. (2017) propose a dynamic ordinal spatial IRT (item response theory) model that allows for inter-temporal comparisons, but their model

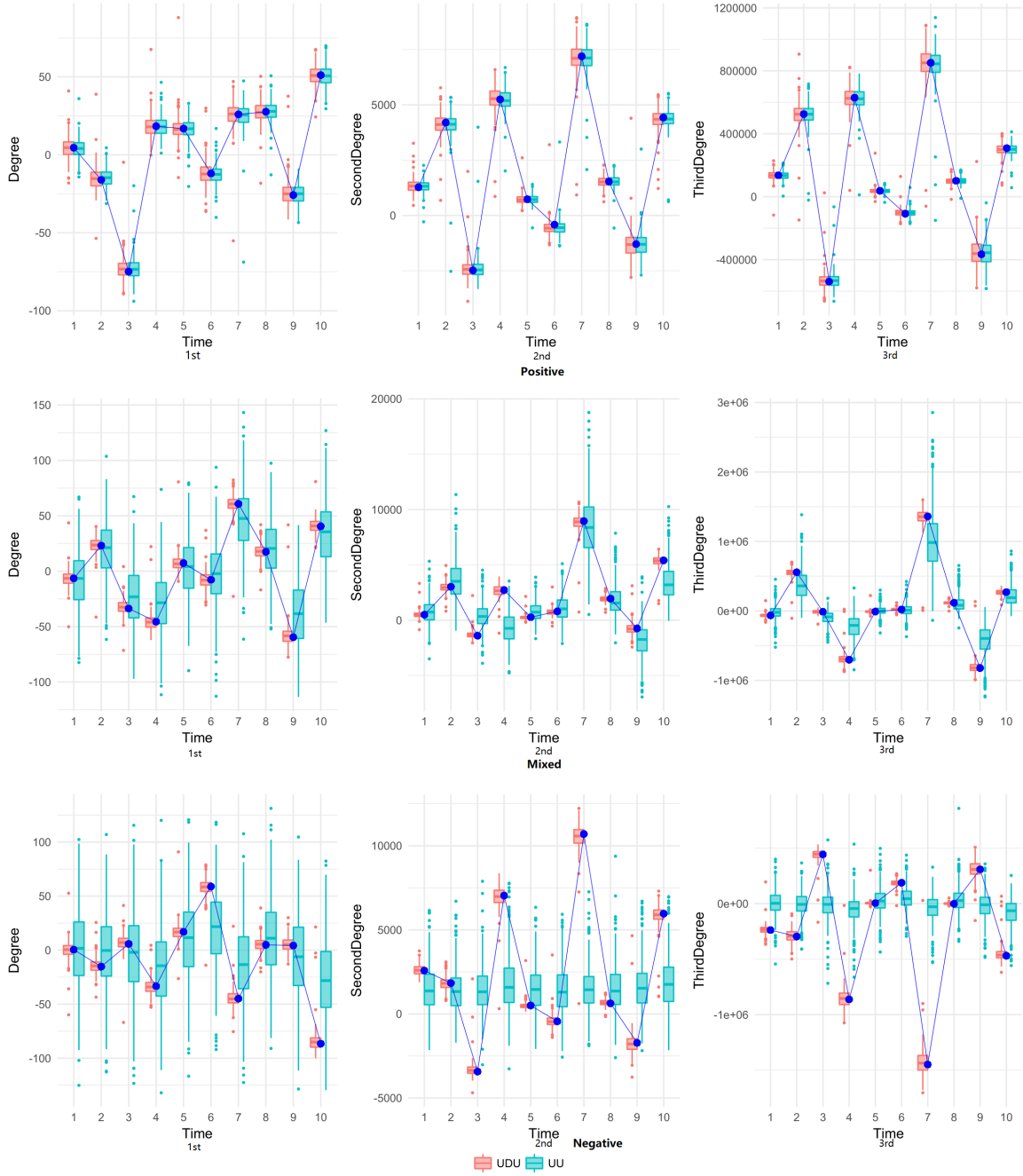


Figure 2: Boxplots of 500 posterior predictive degree statistics in the first (*left*), second (*center*), and third (*right*) moments corresponding to positive (*upper*), mixed (*middle*), and negative (*lower*) transivities: the DAME (red) and the  $u'u$  (green) models are shown with the dots representing the observed statistics.

limits the temporal dependence to be lag 1 (i.e., the Markovian assumption—votes at time  $(t + 1)$  are only dependent on votes at time  $t$ ). Second, although the researchers have viewed “voting” as dyadic behavior and have thus used dyadic similarity indicators such as affinity or S scores (Gartzke, 1998; Signorino and Ritter, 1999), to our knowledge, the United Nations voting data have never been analyzed using network models. Third, higher order dependence (e.g., transitivity and stochastic equivalence) has not been investigated despite the fact that voting decisions are not limited to dyadic relations—country A’s decision to vote along with country B might well be influenced by a country

C’s decision.

We would like to answer the following questions:

- What factors are associated with how countries vote? How do those associations change over time?
- Which countries behave differently, either more likely to vote with others or less likely to vote with others? How do those behaviors change over time?
- Beyond those observed factors, are there any other unobserved alliances that contribute to countries’ voting behavior? How do those alliances change over time?

We consider the time period between 1983-2014, which covers important international events such as the cold war and Iraq war. We first determine the countries to be included in this analysis by the availability of a set of predictors, such as polity score and GDP. We drop countries that have at least one predictor with more than 10 years of missing data. All of the remaining missing values of the predictors are imputed using the data from previous years. This results in 97 countries in total, and the full list of countries with their abbreviations is provided in Appendix C. The voting data are obtained from Voeten (2013). We use the subset of the votes called ‘important votes’, identified by the State Department as “votes on issues which directly affected important United States interests and on which the United States lobbied extensively.” For example, in 2001, important votes include ‘Israeli Actions in the Occupied Territories’, ‘Peaceful Settlement of the Question of Palestine’, ‘U.S. Embargo Against Cuba’, and ‘Nuclear Disarmament’. More can be found on <https://www.state.gov/voting-practices-in-the-united-nations/>. The number of important votes on average is 12 per year, ranging from 6 to 28. We only use important votes because non-important votes show high agreement rate over the time period (1983–2014) without much variation. Annual average voting agreement rates for non-important votes are provided in Appendix D.

Each vote has three categories: Y = “yes” or approval for an issue; A = “abstain”; and N = “no” or disapproval for an issue. For the  $k$ th vote, we define the  $ij$ th entry of the vote-specific undirected agreement network as  $y_{ij}^k = 1$  if country  $i$  and country  $j$  voted Y-Y, N-N, or A-A;  $y_{ij}^k = 0$  if they voted Y-N;  $y_{ij}^k = 0.5$  if they voted Y-A or N-A; and  $y_{ij}^k = NA$  if not both of them voted. Then the annual voting agreement index between two countries  $i$  and  $j$  in year  $t$  is

$$Y_{ijt} = \frac{\sum_k y_{ijt}^k}{\text{Number of votes } i \text{ and } j \text{ both participated in year } t}.$$

Therefore, our response  $\mathbf{Y} = \{\mathbf{Y}^1, \dots, \mathbf{Y}^{32}\}$  is an  $97 \times 97 \times 32$  dimensional array taking values between 0 and 1.

Table 1 illustrates the lagged degree correlation (similar to the lag-1 degree correlation defined in Equation 5) of the observed dataset to measure how strongly the United Nations voting data are correlated over time. The correlation seems to be strong and lingers quite a few years. Under an AR(1) model, the expected auto-correlations for lag 2 and 3 would be  $(0.732)^2 = 0.536$  and  $(0.732)^3 = 0.392$  respectively. Therefore, it seems appropriate to use a non-Markov model.

Lag	1	2	3	4	5	6	7	8	9	10
DC	0.732	0.623	0.513	0.435	0.395	0.315	0.263	0.158	0.164	0.203

Table 1: Lagged degree correlation (DC) of the United Nations voting data for  $l = 1, \dots, 10$ .

Next, we construct  $P = 6$  covariates  $\mathbf{X}$  from the Correlates of War (COW) data (Gibler, 2008), Polity IV data (Marshall et al., 2014), the International Monetary Fund (IMF)’s Direction of Trade Statistics (DOTS) and International Financial Statistics (IFS) data. For  $p = 1, \dots, P$ , the explanatory variable  $X_{ijp}^t$  is the following:

1.  $X_{ij1}^t$ : intercept, included to account for the baseline degree of agreement.
2.  $X_{ij2}^t$ : log of the geographic distance between the capital cities of country  $i$  and country  $j$ .
3.  $X_{ij3}^t$ : 1 if country  $i$  and country  $j$  have a formal alliance including mutual defense pacts, non-aggression treaties, and ententes at time  $t$ , and 0 otherwise.

4.  $X_{ij4}^t$ : absolute difference in polity score between country  $i$  and country  $j$  at time  $t$ <sup>1</sup>.
5.  $X_{ij5}^t$ : index of economic dependence using bilateral trade weighted by each country’s gross domestic product (GDP), as defined in Gartzke (2000). That is,

$$X_{ij5}^t = \min\left(\frac{\text{Trade}_{ijt}}{\text{GDP}_{it}}, \frac{\text{Trade}_{ijt}}{\text{GDP}_{jt}}\right).$$

6.  $X_{ij6}^t$ : indicator of whether country  $i$  and country  $j$  share the official language.

By definition, all covariates are symmetric (i.e.,  $X_{ijp}^t = X_{jip}^t$ ). Two variables— $\log(\text{distance})$  and common language—are time-invariant covariates, although their coefficients varies over time. The rest are time varying covariates. Correlations between the covariates are summarized in Appendix D.

We specify the matrix of availability  $\mathbf{A}$  introduced in Section 2.3 to reflect some countries’ non-participation in the United Nations General Assembly (UNGA):

1. North Korea (PRK) has structural missing values from  $t = 1$  to  $t = 8$  because North Korea did not vote until North Korea and South Korea were simultaneously admitted to the United Nations in 1991.
2. South Korea (ROK) has structural missing values from  $t = 1$  to  $t = 8$  because South Korea did not vote until North Korea and South Korea were simultaneously admitted to the United Nations in 1991.
3. Russia (RUS) has structural missing values from  $t = 1$  to  $t = 9$  because Russia succeeded the Soviet Union’s seat, including its permanent membership on the Security Council in the United Nations, after the dissolution of the Soviet Union in 1991.
4. Iraq (IRQ) has structural missing values from  $t = 13$  to  $t = 21$  because Iraq did not participate in the UNGA roll-call votes from 1995 to 2003. Under the rule of Saddam, Iraq had been under severe sanctions from the international community, including the United Nations, since 1990.

Any missing values corresponding to a country’s missing period are treated as structural missing values. As explained in Section 2.3, other missing values are treated as random missing and thus imputed.

## 4.2 Model Validation

Before presenting the results, we would like to check the fit of the DAME model to the data and have some confidence in the results. We validate the model from two aspects. First, we examine the overall goodness-of-fit in a similar fashion as in AMEN. We generate posterior predictive datasets from the fitted model. Then year by year, we compare the mean and standard deviation of the first, second, and third order moment statistics (as defined in the previous section) of the generated datasets with the observed one. Figure 3 shows one of the comparisons. We can see that the model resembles those features of the observed data well. For the complete set of posterior predictive checks, see <https://github.com/bomin8319/DAME>.

Then we investigate the necessity of including each component in the model. Specifically, we fit the model with four different specifications: 1) one with additive and multiplicative effects (DAME), 2) one with only multiplicative effects (ME), 3) one with only additive effects (AE), and 4) one without any random effects (NO). Each of the four specifications uses all six edge covariates in Section 4.1. Figure 4 depicts the degree statistics constructed from 500 different posterior predictive samples. Here we take Uruguay (URU) as an example to discuss the general findings. First of all, we see the bias correcting effect of including additive effects (AE), compared to the model with no random effects (NO). Next, when we compare models with only additive effects (AE) and only multiplicative effects (ME), the multiplicative effects model shows significantly narrower credible intervals. Lastly,

---

<sup>1</sup>Polity IV data contain coded annual information on the level of democracy for various countries, and a polity score ranges from -10 to +10, with -10 to -6 corresponding to autocracies, -5 to 5 corresponding to anocracies, and 6 to 10 to democracies.

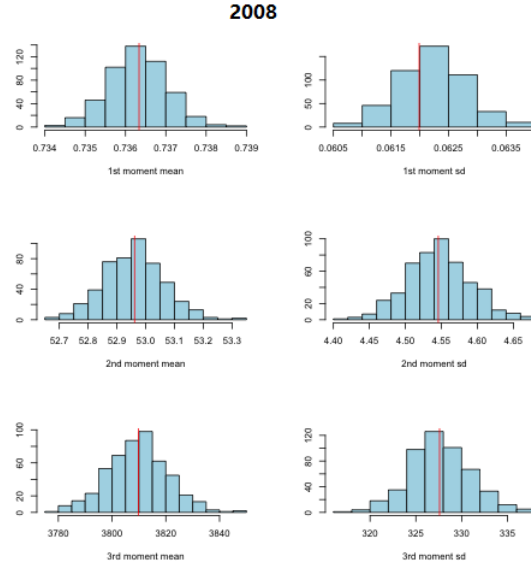


Figure 3: Posterior predictive distribution of the mean and standard deviations of first, second, and third order moment statistics. The observed statistics are represented by the vertical lines.

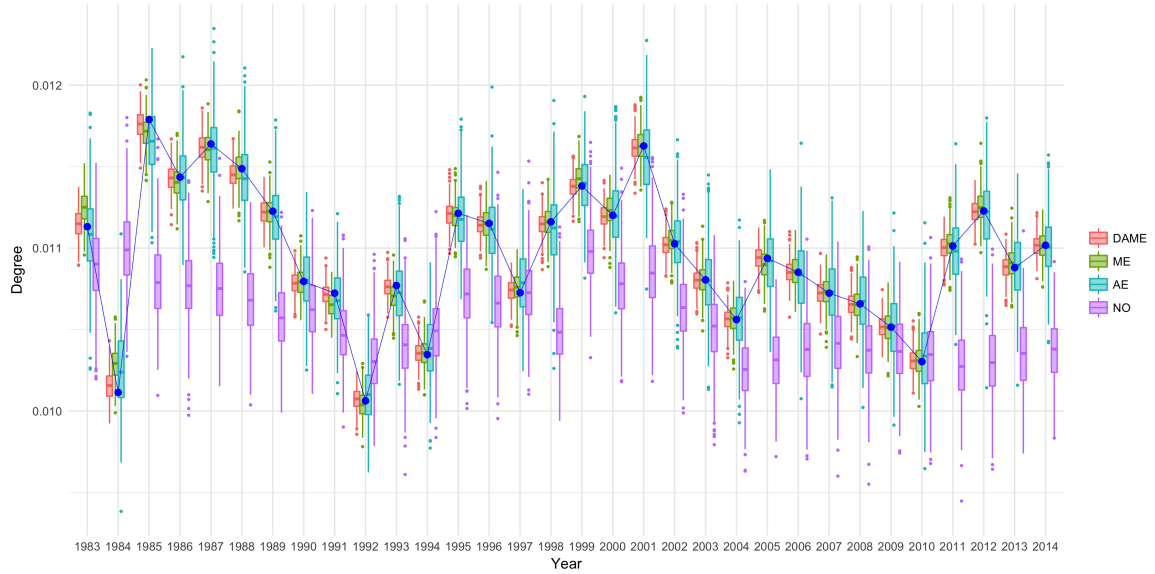


Figure 4: Boxplots of 500 posterior predictive degree statistics for Uruguay (URU): the DAME (*red*), ME (*green*), AE (*blue*), and NO (*purple*) models are shown with the dots representing the country's observed statistics.

our model with both additive and multiplicative effects (DAME) outperforms the ME model in terms of both accuracy and precision. To be specific, the DAME model corrects the bias in the ME model by incorporating node-specific additive effects. Overall, not only does the DAME model provide the most accurate estimates over time, but it also yields the narrowest 95% credible intervals among the four. Specifically, the sum of squared errors (SSE) over all posterior samples  $k = 1, \dots, 500$ , countries  $i = 1, \dots, 97$ , and timepoints  $t = 1, \dots, 32$  (i.e.,  $SSE = \sum_{t=1}^{32} \sum_{i=1}^{97} \sum_{k=1}^{500} (Y_{ik}^t - \hat{Y}_{ik}^t)^2$ ) are 1.864 for the NO model, 0.074 for the AE model, 0.017 for the ME model, and 0.009 for the DAME model. These outcomes justifies the inclusion of all the components in our model.

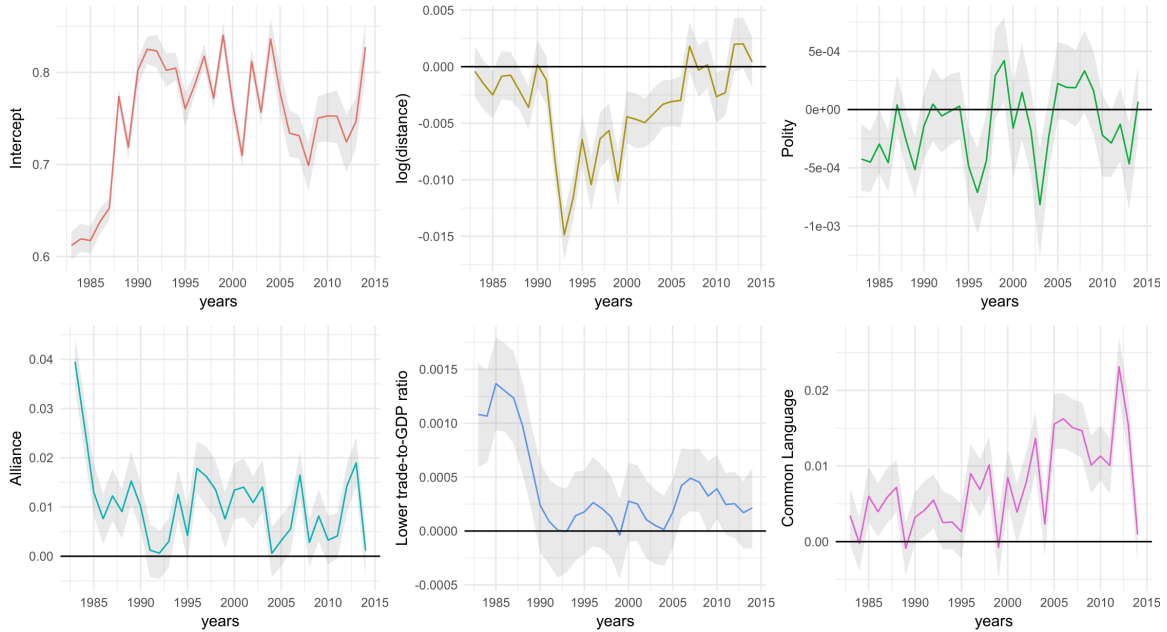


Figure 5: Posterior mean estimates for the fixed effect coefficients  $\beta$  (colored line): Intercept,  $\log(\text{distance})$ , Alliance, Polity difference, Lower trade-to-GDP ratio, and Common Language, and their corresponding 95% credible intervals (grey areas).

### 4.3 Results and Interpretation

We apply the DAME model to the United Nations General Assembly voting data. We fix the dimension of the multiplicative effects to be  $R = 2$  based on some preliminary experiments, where increasing the dimension does not significantly improve the model fitting. For instance, the estimated eigenvalue  $d_3^t \approx 0$  for every  $t = 1, \dots, T$ . In this section, we present the results based on 30,000 Gibbs iterations. Due to strong autocorrelation among the parameters, we tuned the chain with a burn-in of 5,000 and thinned the iterations by keeping every 50<sup>th</sup> sample. All model parameters, including the GP parameters  $(\kappa, \tau)$ , are estimated according to Section 2.2, using the hyperparameters  $(a, b) = (2, 1)$  and  $\gamma = 5$ .

Figure 5 shows the posterior mean estimates of the fixed effects coefficients  $\{\beta_p\}_{p=1}^P$  with their corresponding 95% credible intervals. Overall, the effects of the covariates on the United Nations voting behavior change substantially over time, especially in the cases of geographic distance and trade-to-GDP ratio. Most importantly, the “critical junction” for these temporal changes seems to be around the end of Cold War, that is, the late 1980s and early 1990s. For instance, the middle panel of the top row reveals the pattern of influence of geographic distance on voting behavior. The gravity model (Leibenstein, 1966; Rodrigue et al., 2016) suggests that bilateral flows (e.g., trade, migration, and even in the case of portfolio investment) between two countries is a negative function of the distance between them. We see an overall negative coefficient for geographic distance which is consistent with the gravity model. However, the negative effect of geographic distance is less significant after the early 1990s. It is likely that the votes in the United Nations were much more influenced by the overall ideological conflicts between the Soviet Union plus its satellites and the Western camp so the effect of geographical distance was weakened during the Cold War. Moreover, regarding the effect of polity—or distance in polity as we operationalize this variable—the result suggests that in general the political regime similarity does not often result in higher agreement in the United Nations General Assembly, at least for a few time periods included in the study, e.g., 1990–1995, 1997–2002, and 2005–2010. Scholars in the liberal tradition of international relations have long been arguing for shared norms, values and preferences between democracies; what the result here suggests is that such similarity in preferences seem to be not sufficiently strong enough to sway countries’

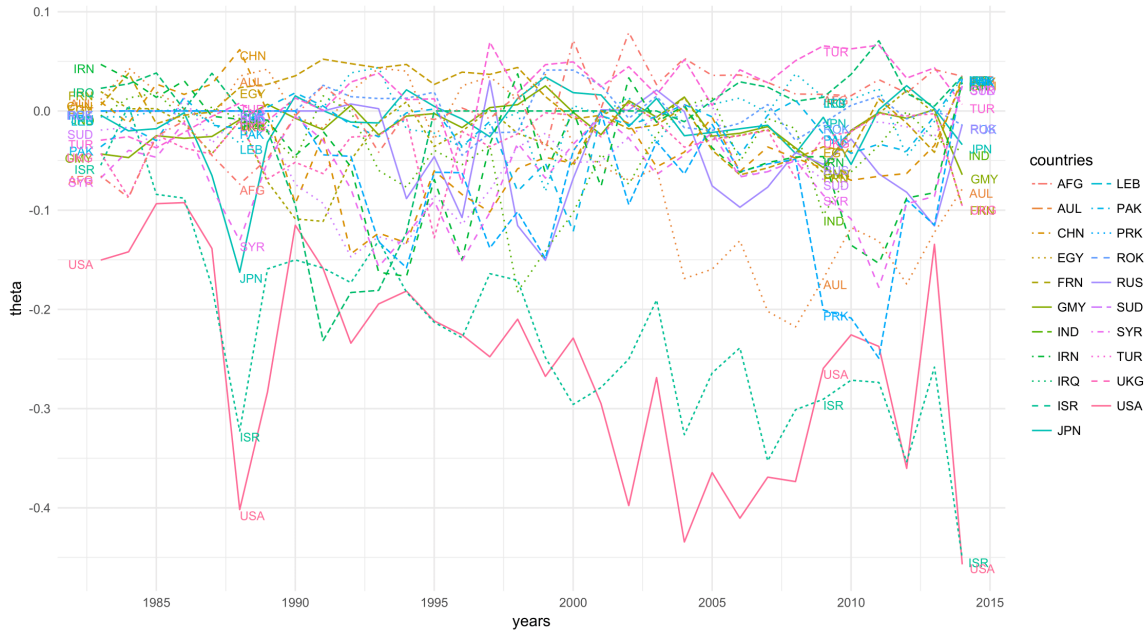


Figure 6: Posterior mean estimates for the additive random effect estimates  $\theta$ .

votes in the United Nations General Assembly, at least in the case of important votes and when we account for the other factors in the model. Moreover, as we expect, having alliances, active trade, and common languages all have positive effects to vote similarly.

After controlling for the observed covariates, we move on to the analysis of random effects. For clear visualization, we only present the result from 21 countries, where the countries are chosen based on the most active countries during the ten year period from 2004 to 2014 (Hoff, 2015). The 21 most active countries are marked with \* in Appendix C. Figure 6 shows the posterior mean estimates of each country’s additive random effects, that is, its node-specific time-varying intercepts  $\theta_i^t$ . Here, the United States (USA) and Israel (ISR) stand out with large negative additive random effects, suggesting that these two countries are less likely to cast the same votes as the rest of the countries. Considering that the majority of votes are “yes”, the two countries are more likely to vote for “no” in general.

Finally, we provide the estimated 2-dimensional multiplicative effects of the 21 countries. To determine the posterior distribution of  $\mathbf{u}$  without identifiability issues, we calculate an eigendecomposition on every posterior sample of the multiplicative effect matrix  $\mathbf{u}'\mathbf{D}\mathbf{u}$ , and let  $\mathbf{D}$  be the diagonal matrix of eigenvalues and  $\mathbf{u}$  be the corresponding eigenvectors. For the UN voting data, we find that both of the eigenvalues are positive over the time period, which implies positive homophily in the countries’ latent positions after accounting for the observed predictors and individual differences. Figure 7 shows the posterior mean and 95% credible band of the estimated  $\mathbf{D}$ .

We then apply a Procrustes transformation on each posterior estimate of  $\mathbf{u}$  and multiply by  $\sqrt{\mathbf{D}}$ , and obtain the posterior mean estimates and 95% credible regions of  $\mathbf{u}_i\sqrt{\mathbf{D}}$ , for all  $i = 1, \dots, N$ . In Figure 8, we see interesting patterns of clustering of countries over time. For example, in 1984, USA and China (CHN) shared very similar latent positions – the closest compared to latent positions in all other years – this reflects the historical fact that after the normalization of foreign policies between the two countries in 1978, USA and China had a close relationship in foreign policies all the way till the end of the Cold War when the common enemy, i.e., the Soviet Union, collapsed. Indeed, when we look at unreported yearly latent plots for 1985-1989, USA and China are always close. This seems to have changed in 1990 when China’s position in the latent space became more isolated from other countries. This might reflect the relatively unfavorable foreign relations China experienced since the event unfolded in June of 1989. Also interestingly, ever since the mid 1990s, Israel (ISR) has always

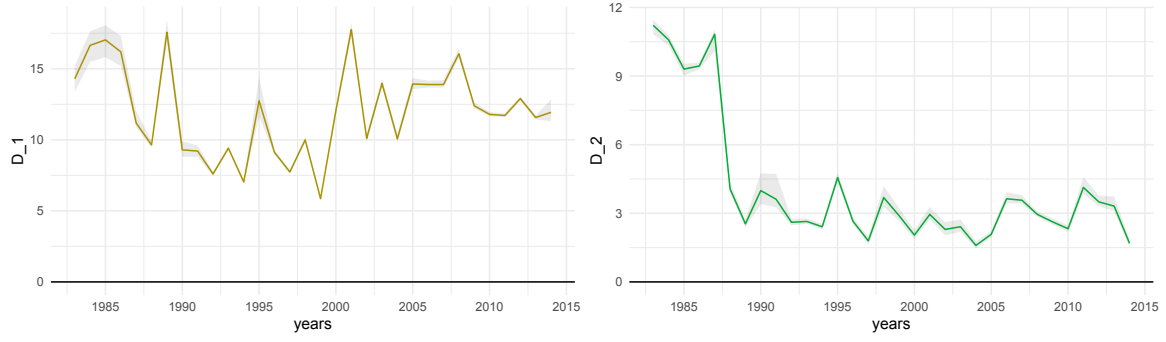


Figure 7: Posterior mean and 95% credible band of the eigenvalue  $\mathbf{D}$ .

been close to the USA in the latent space, suggesting a special foreign policy relationship between these two countries. <sup>2</sup>

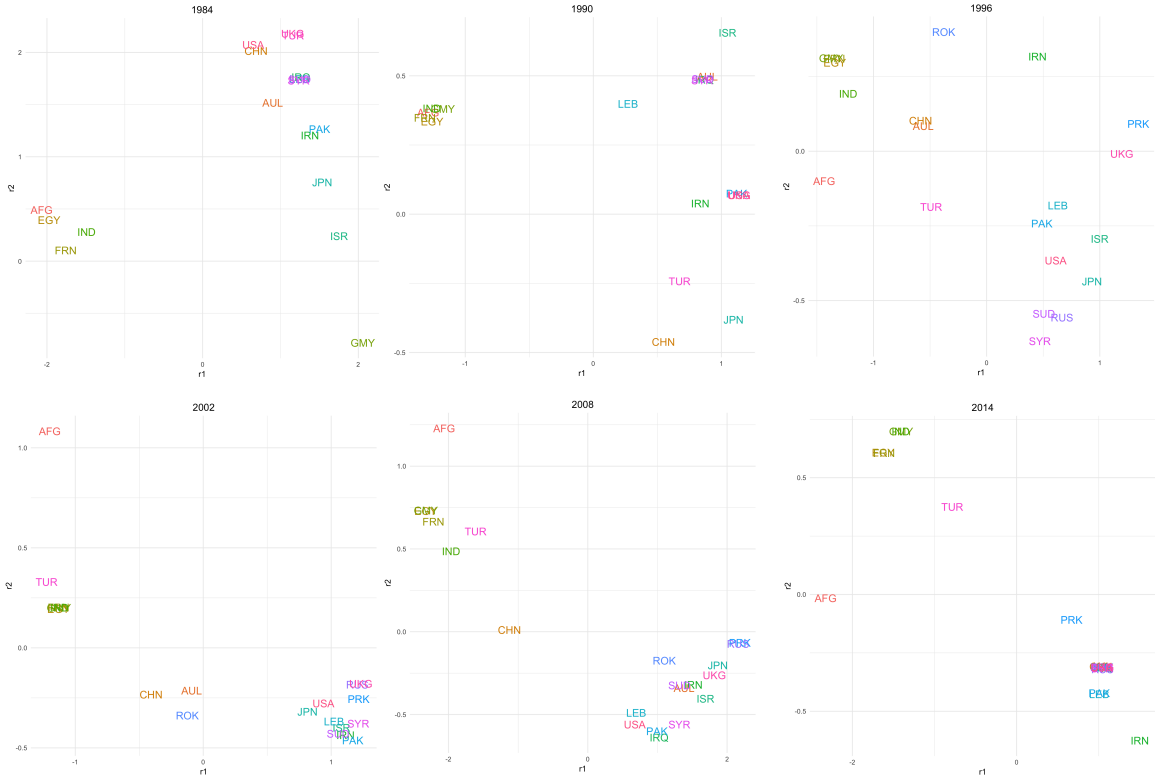


Figure 8: Posterior mean estimates for the multiplicative random effects and their corresponding 95% credible regions for the 21 selected countries for every 6 years between 1984 and 2014.

## 5 Discussion

As an extension of the additive and multiplicative effects (AME) model, the dynamic additive and multiplicative effects (DAME) network model can flexibly learn the underlying time-varying structure in dynamic networks, while inferring the effects of node-specific and dyad-specific latent variables.

<sup>2</sup>The dataset and codes used in this paper can be found at <https://github.com/bomin8319/DAME>.

Accounting for the correlation structure of the networks makes better use of dynamic networks than modeling them as separate network snapshots. The visualization of the model-estimated time-varying parameters provides an effective temporal trend analysis of dynamic networks, as well as the descriptive visualization of higher-order dependence over time. In modeling the United Nations voting behavior, which is the example that has motivated our model, the estimated additive and multiplicative effects and their changes over time reveal interesting and meaningful foreign policy positions and latent alliances of various countries, even after controlling for other known predictors that are considered critical in the studies of international relations. Even though this particular data display positive homophily over time, we have demonstrated with careful simulation studies that having the flexibility of allowing both positive and negative homophily is beneficial, especially before analyzing the data and knowing the patterns. Therefore, the methodology proposed here goes beyond this particular example and can be applied to a wide range of applications.

In this application, the main research question is to study the associated factors in general voting agreement among UN nations. If researchers are interested in the determining factors in changes of voting behaviors, we could include  $Y_{t-1}$  in the model, as in Friel et al. (2016). Given the evidence found in the data that the current year’s outcome highly depends on the previous year, this additional term could also improve the goodness of fit of the model.

Although we illustrate the entire framework in the context of symmetric or undirected networks, our model can be easily extended to allow directed networks, following the additive and multiplicative effects model for the directed network (Hoff, 2019). Furthermore, the approach can be applied to binary and ordinal network data with appropriate link functions. Finally, considering the recent explosion of network dataset with time granularity, future work could be focused on the improvement of model’s computational efficiency. Without applying too many computational tricks (we’ve only considered group updating parameters, random order of updating the latent variables, and thinning), our current MCMC algorithm mixes slowly and takes about 20 hours to fully converge, which limits its scalability. Development of promising inferential and computational approaches that can accommodate huge networks that span long periods of time will surely broaden the range of our model applicability.

## References

- Airoldi, E. M., Blei, D. M., Fienberg, S. E., and Xing, E. P. (2008). Mixed membership stochastic blockmodels. *Journal of Machine Learning Research*, 9(Sep):1981–2014.
- Bailey, M. A., Strezhnev, A., and Voeten, E. (2017). Estimating dynamic state preferences from united nations voting data. *Journal of Conflict Resolution*, 61(2):430–456.
- Bearce, D. H. and Bondanella, S. (2007). Intergovernmental organizations, socialization, and member-state interest convergence. *International Organization*, 61(4):703–733.
- Durante, D. and Dunson, D. B. (2014). Nonparametric bayes dynamic modelling of relational data. *Biometrika*, 101(4):883–898.
- Frank, O. and Strauss, D. (1986). Markov graphs. *Journal of the American Statistical Association*, 81(395):832–842.
- Friel, N., Rastelli, R., Wyse, J., and Raftery, A. E. (2016). Interlocking directorates in irish companies using a latent space model for bipartite networks. *Proceedings of the National Academy of Sciences*, 113(24):6629–6634.
- Gartzke, E. (1998). Kant we all just get along? opportunity, willingness, and the origins of the democratic peace. *American Journal of Political Science*, 42:1–27.
- Gartzke, E. (2000). Preferences and the democratic peace. *International Studies Quarterly*, 44(2):191–212.
- Gibler, D. M. (2008). *International military alliances, 1648-2008*. CQ Press.

- Hanneke, S., Fu, W., Xing, E. P., et al. (2010). Discrete temporal models of social networks. *Electronic Journal of Statistics*, 4:585–605.
- Ho, Q., Song, L., and Xing, E. (2011). Evolving cluster mixed-membership blockmodel for time-varying networks. *Journal of Machine Learning Research: Workshop and Conference Proceedings*, 15:342–350.
- Hoff, P. (2008). Modeling homophily and stochastic equivalence in symmetric relational data. In Platt, J. C., Koller, D., Singer, Y., and Roweis, S. T., editors, *Advances in Neural Information Processing Systems 20*, pages 657–664.
- Hoff, P. (2019). Additive and multiplicative effects network models. *Statistical Science*. to appear.
- Hoff, P. D. (2005). Bilinear mixed-effects models for dyadic data. *Journal of the American Statistical Association*, 100(469):286–295.
- Hoff, P. D. (2015). Multilinear tensor regression for longitudinal relational data. *The Annals of Applied Statistics*, 9(3):1169.
- Hoff, P. D., Raftery, A. E., and Handcock, M. S. (2002). Latent space approaches to social network analysis. *Journal of the American Statistical Association*, 97(460):1090–1098.
- Karrer, B. and Newman, M. E. J. (2011). Stochastic blockmodels and community structure in networks. *Physical Review E*, 83(1):016107.
- Kim, B., Lee, K. H., Xue, L., Niu, X., et al. (2018). A review of dynamic network models with latent variables. *Statistics Surveys*, 12:105–135.
- Krivitsky, P. N. and Handcock, M. S. (2014). A separable model for dynamic networks. *Journal of the Royal Statistical Society. Series B, Statistical Methodology*, 76 1:29–46.
- Leibenstein, H. (1966). Shaping the world economy: Suggestions for an international economic policy.
- Marshall, M. G., Jagers, K., and Gurr, T. R. (2014). Polity iv annual time-series, 1800–2013. *Center for International Development and Conflict Management at the University of Maryland College Park*.
- Matias, C. and Miele, V. (2017). Statistical clustering of temporal networks through a dynamic stochastic block model. *Journal of the Royal Statistical Society: Series B (Statistical Methodology)*, 79(4):1119–1141.
- Mattes, M., Leeds, B. A., and Carroll, R. (2015). Leadership turnover and foreign policy change: Societal interests, domestic institutions, and voting in the United Nations. *International Studies Quarterly*, 59(2):280–290.
- Nowicki, K. and Snijders, T. A. B. (2001). Estimation and prediction for stochastic blockstructures. *Journal of the American Statistical Association*, 96(455):1077–1087.
- Rasmussen, C. E. (2003). Gaussian processes in machine learning. In *Summer School on Machine Learning*, pages 63–71. Springer.
- Robins, G. and Pattison, P. (2001). Random graph models for temporal processes in social networks. *The Journal of Mathematical Sociology*, 25(1):5–41.
- Rodrigue, J.-P., Comtois, C., and Slack, B. (2016). *The geography of transport systems*. Routledge.
- Sarkar, P. and Moore, A. W. (2006). Dynamic social network analysis using latent space models. In *Advances in Neural Information Processing Systems*, pages 1145–1152.
- Sarkar, P., Siddiqi, S. M., and Gordon, G. J. (2007). A latent space approach to dynamic embedding of co-occurrence data. In *Artificial Intelligence and Statistics*, pages 420–427.
- Sewell, D. K. and Chen, Y. (2015). Latent space models for dynamic networks. *Journal of the American Statistical Association*, 110(512):1646–1657.

- Sewell, D. K. and Chen, Y. (2016). Latent space models for dynamic networks with weighted edges. *Social Networks*, 44:105–116.
- Signorino, C. S. and Ritter, J. M. (1999). Tau-b or not tau-b: Measuring the similarity of foreign policy positions. *International Studies Quarterly*, 43(1):115–144.
- Snijders, T. A. and Nowicki, K. (1997). Estimation and prediction for stochastic blockmodels for graphs with latent block structure. *Journal of Classification*, 14:75–100.
- Snijders, T. A., Van de Bunt, G. G., and Steglich, C. E. (2010). Introduction to stochastic actor-based models for network dynamics. *Social networks*, 32(1):44–60.
- Snijders, T. A. B. (2001). The statistical evaluation of social network dynamics. *Sociological Methodology*, 31(1):361–395.
- Snijders, T. A. B., Steglich, C., and Schweinberger, M. (2007). Modeling the co-evolution of networks and behavior. In van Montfort, K., Oud, J., and Satorra, A., editors, *Longitudinal models in the behavioral and related sciences*, pages 41–71. Lawrence Erlbaum Associates.
- Voeten, E. (2000). Clashes in the assembly. *International organization*, 54(2):185–215.
- Voeten, E. (2004). Resisting the lonely superpower: Responses of states in the united nations to us dominance. *The Journal of Politics*, 66(3):729–754.
- Voeten, E. (2013). Data and analyses of voting in the un general assembly. In Reinalda, B., editor, *Routledge Handbook of International Organization*. Routledge. Available at SSRN: <http://ssrn.com/abstract=2111149>.
- Wendt, A. (1994). Collective identity formation and the international state. *American political science review*, 88(2):384–396.
- Xing, E. P., Fu, W., and Song, L. (2010). A state-space mixed membership blockmodel for dynamic network tomography. *The Annals of Applied Statistics*, 4(2).
- Xu, K. S. and Hero, A. O. (2013). Dynamic stochastic blockmodels: Statistical models for time-evolving networks. In *International Conference on Social Computing, Behavioral-Cultural Modeling, and Prediction*, pages 201–210. Springer.
- Yang, T., Chi, Y., Zhu, S., Gong, Y., and Jin, R. (2011). Detecting communities and their evolutions in dynamic social networks—a bayesian approach. *Machine learning*, 82(2):157–189.

# Appendices

## A Derivations of Full Conditional Distributions

The noise error variance  $\sigma_e^2$  has a conditional inverse-gamma distribution with parameters as derived below:

$$\begin{aligned}
\Pr(\sigma_e^2 | \mathbf{Y}, k_\sigma, \theta_\sigma) &\propto \Pr(\mathbf{Y} | \mathbf{X}, \boldsymbol{\beta}, \mathbf{a}, \mathbf{d}, \mathbf{u}, \sigma_e^2) \times \Pr(\sigma_e^2 | k_\sigma, \theta_\sigma) \\
&\propto \prod_{t=1}^T \prod_{i>j} (\sigma_e^2)^{-\frac{1}{2}} \exp\left\{ -\frac{1}{2\sigma_e^2} \|y_{ij}^t - (\sum_{p=1}^P \beta_p^t X_{ijp}^t + a_i^t + a_j^t + \mathbf{u}_i^{t'} \mathbf{D}^t \mathbf{u}_j^t)\|^2 \right\} \times (\sigma_e^2)^{-k_\sigma - 1} \exp\left\{ \frac{1}{\sigma_e^2} \theta_\sigma \right\} \\
&= (\sigma_e^2)^{-\frac{T}{2} \cdot \frac{N(N-1)}{2} - k_\sigma - 1} \times \exp\left\{ -\frac{1}{\sigma_e^2} \left( \frac{1}{2} \sum_{t=1}^T \sum_{i>j} \|y_{ij}^t - (\sum_{p=1}^P \beta_p^t X_{ijp}^t + a_i^t + a_j^t + \mathbf{u}_i^{t'} \mathbf{D}^t \mathbf{u}_j^t)\|^2 + \theta_\sigma \right) \right\} \\
&\sim \mathcal{IG}\left(\frac{T \cdot N(N-1)}{4} + k_\sigma, \frac{1}{2} \sum_{t=1}^T \sum_{i>j} (E_{ij}^t)^2 + \theta_\sigma\right)
\end{aligned}$$

The fixed effect coefficient  $\boldsymbol{\beta}_p$  (for  $p = 1, \dots, P$ ) has a conditional multivariate normal distribution with parameters as derived below:

$$\begin{aligned}
\Pr(\boldsymbol{\beta}_p | \mathbf{Y}, \mathbf{X}, \kappa_p^\beta, \tau_p^\beta) &\propto \Pr(\mathbf{Y} | \mathbf{X}, \boldsymbol{\beta}_p, \boldsymbol{\beta}_{[-p]}, \mathbf{a}, \mathbf{d}, \mathbf{u}, \sigma_e^2) \times \Pr(\boldsymbol{\beta}_p | \kappa_p^\beta, \tau_p^\beta) \\
&\propto \prod_{i>j} \exp\left\{ -\frac{1}{2\sigma_e^2} \|\mathbf{E}_{ij[-p]} - \mathbf{X}_{ijp} \boldsymbol{\beta}_p\|^2 \right\} \times \exp\left\{ -\frac{1}{2} (\boldsymbol{\beta}_p' (\Sigma_p^\beta)^{-1} \boldsymbol{\beta}_p) \right\} \\
&\quad \text{where } \mathbf{E}_{ij[-p]} = \{E_{ij[-p]}^t\}_{t=1}^T \text{ (with } E_{ij[-p]}^t = E_{ij}^t + \beta_p^t X_{ijp}^t) \text{ and } \mathbf{X}_{ijp} = \{X_{ijp}^t\}_{t=1}^T \\
&\propto \exp\left\{ -\frac{1}{2\sigma_e^2} \left( \sum_{i>j} -2(\mathbf{E}_{ij[-p]} \mathbf{X}_{ijp})' \boldsymbol{\beta}_p + \boldsymbol{\beta}_p' (\text{diag}(\sum_{i>j} \mathbf{X}_{ijp}^2)) \boldsymbol{\beta}_p \right) \right\} \times \exp\left\{ -\frac{1}{2} (\boldsymbol{\beta}_p' (\Sigma_p^\beta)^{-1} \boldsymbol{\beta}_p) \right\} \\
&\propto \exp\left\{ -\frac{1}{2} \left( \boldsymbol{\beta}_p' ((\Sigma_p^\beta)^{-1} + \frac{\text{diag}(\sum_{i>j} \mathbf{X}_{ijp}^2)}{\sigma_e^2}) \boldsymbol{\beta}_p - \frac{2}{\sigma_e^2} (\sum_{i>j} (\mathbf{E}_{ij[-p]} \mathbf{X}_{ijp})' \boldsymbol{\beta}_p) \right) \right\} \\
&\sim \mathcal{N}_T(\tilde{\boldsymbol{\mu}}_{\beta_p}, \tilde{\Sigma}_{\beta_p}), \\
&\quad \text{where } \tilde{\Sigma}_{\beta_p} = \left( (\Sigma_p^\beta)^{-1} + \frac{\text{diag}(\{\sum_{i>j} X_{ijp}^2\}_{t=1}^T)}{\sigma_e^2} \right)^{-1} \text{ and } \tilde{\boldsymbol{\mu}}_{\beta_p} = \left( \frac{\{\sum_{i>j} (\mathbf{E}_{ij[-p]}^t \mathbf{X}_{ijp}^t)\}_{t=1}^T}{\sigma_e^2} \right) \tilde{\Sigma}_{\beta_p}.
\end{aligned}$$

The additive random effect  $\mathbf{a}_i$  (for  $i = 1, \dots, N$ ) has a conditional multivariate normal distribution with parameters as derived below:

$$\begin{aligned}
\Pr(\mathbf{a}_i | \mathbf{Y}, \kappa^a, \tau^a) &\propto \prod_{j \neq i} \Pr(\mathbf{Y} | \mathbf{X}, \boldsymbol{\beta}, \mathbf{a}_i, \mathbf{a}_{[-i]}, \mathbf{d}, \mathbf{u}, \sigma_e^2) \times \Pr(\mathbf{a}_i | \kappa^a, \tau^a) \\
&\propto \prod_{j \neq i} \exp\left\{ -\frac{1}{2\sigma_e^2} \|\mathbf{E}_{ij[-i]} - \mathbf{a}_i\|^2 \right\} \times \exp\left\{ -\frac{1}{2} (\mathbf{a}_i' (\Sigma^a)^{-1} \mathbf{a}_i) \right\} \\
&\quad \text{where } \mathbf{E}_{ij[-i]} = \{E_{ij[-i]}^t\}_{t=1}^T \text{ with } E_{ij[-i]}^t = E_{ij}^t + \mathbf{a}_i^t \\
&\propto \exp\left\{ -\frac{1}{2\sigma_e^2} \left( \sum_{j \neq i} -2(\mathbf{E}_{ij[-i]} \mathbf{a}_i + \mathbf{a}_i' (\sum_{j \neq i} I_T) \mathbf{a}_i) \right) \right\} \times \exp\left\{ -\frac{1}{2} (\mathbf{a}_i' (\Sigma^a)^{-1} \mathbf{a}_i) \right\} \\
&\propto \exp\left\{ -\frac{1}{2} \left( \mathbf{a}_i' ((\Sigma^a)^{-1} + \frac{(N-1)I_T}{\sigma_e^2}) \mathbf{a}_i - \frac{2}{\sigma_e^2} (\sum_{j \neq i} (\mathbf{E}_{ij[-i]} \mathbf{a}_i)) \right) \right\} \\
&\sim \mathcal{N}_T(\tilde{\boldsymbol{\mu}}_{a_i}, \tilde{\Sigma}_{a_i}), \\
&\quad \text{where } \tilde{\Sigma}_{a_i} = \left( (\Sigma^a)^{-1} + \frac{(N-1)I_T}{\sigma_e^2} \right)^{-1} \text{ and } \tilde{\boldsymbol{\mu}}_{a_i} = \left( \frac{\{\sum_{j \neq i} \mathbf{E}_{ij[-i]}^t\}_{t=1}^T}{\sigma_e^2} \right) \tilde{\Sigma}_{a_i}.
\end{aligned}$$

The latent vector of multiplicative random effect  $\mathbf{u}_{ir}$  (for  $i = 1, \dots, N$  and  $r = 1, \dots, R$ ) has a conditional multivariate normal distribution with parameters as derived below:

$$\begin{aligned}
& \Pr(\mathbf{u}_{ir} | \mathbf{Y}, \kappa_r^u, \tau_r^u) \propto \Pr(\mathbf{Y} | \mathbf{X}, \boldsymbol{\beta}, \mathbf{a}, \mathbf{d}, \mathbf{u}_{ir}, \mathbf{u}_{[-ir]}, \sigma_e^2) \times \Pr(\mathbf{u}_{ir} | \kappa_r^u, \tau_r^u) \\
& \propto \prod_{i=1}^N \prod_{j \neq i} \exp \left\{ -\frac{1}{2\sigma_e^2} \|\mathbf{E}_{ij[-r]} - \mathbf{u}'_{ir} \mathbf{d}_r \mathbf{u}_{jr}\|^2 \right\} \times \exp \left\{ -\frac{1}{2} (\mathbf{u}'_{ir} (\Sigma_r^u)^{-1} \mathbf{u}_{ir}) \right\} \\
& \quad \text{where } \mathbf{E}_{ij[-r]} = \{E_{ij[-r]}^t\}_{t=1}^T \text{ (with } E_{ij[-r]}^t = E_{ij}^t + u_{ir}^t d_r^t u_{jr}^t \text{)} \text{ and } \mathbf{u}'_{ir} \mathbf{d}_r \mathbf{u}_{jr} = \{u_{ir}^t d_r^t u_{jr}^t\}_{t=1}^T \\
& \propto \exp \left\{ -\frac{1}{4\sigma_e^2} \left( \sum_{j \neq i} -2(\mathbf{E}_{ij[-r]} \mathbf{d}_r \mathbf{u}_{jr})' \mathbf{u}_{ir} + \mathbf{u}'_{ir} (\text{diag}(\mathbf{d}_r^2 \sum_{j \neq i} \mathbf{u}_{jr}^2)) \mathbf{u}_{ir} \right) \right\} \times \exp \left\{ -\frac{1}{2} (\mathbf{u}'_{ir} (\Sigma_r^u)^{-1} \mathbf{u}_{ir}) \right\} \\
& \propto \exp \left\{ -\frac{1}{2} \left( \mathbf{u}'_{ir} ((\Sigma_r^u)^{-1} + \frac{1}{2} \times \frac{\text{diag}(\mathbf{d}_r^2 \sum_{j \neq i} \mathbf{u}_{jr}^2)}{\sigma_e^2}) \mathbf{u}_{ir} - \frac{2}{\sigma_e^2} \left( \frac{1}{2} \sum_{j \neq i} (\mathbf{E}_{ij[-r]} \mathbf{d}_r \mathbf{u}_{jr})' \mathbf{u}_{ir} \right) \right) \right\} \\
& \sim \mathcal{N}_T(\tilde{\boldsymbol{\mu}}_{\mathbf{u}_{ir}}, \tilde{\boldsymbol{\Sigma}}_{\mathbf{u}_{ir}}) \\
& \text{where } \tilde{\boldsymbol{\Sigma}}_{\mathbf{u}_{ir}} = \left( (\Sigma_r^u)^{-1} + \frac{\text{diag}(\{(d_r^t)^2 \sum_{j \neq i} (u_{jr}^t)^2\}_{t=1}^T)}{2\sigma_e^2} \right)^{-1} \text{ and } \tilde{\boldsymbol{\mu}}_{\mathbf{u}_{ir}} = \left( \frac{\{\sum_{j \neq i} (E_{ij[-r]}^t d_r^t u_{jr}^t)\}_{t=1}^T}{2\sigma_e^2} \right) \tilde{\boldsymbol{\Sigma}}_{\mathbf{u}_{ir}}.
\end{aligned}$$

The eigenvalue part of multiplicative random effect  $\mathbf{d}^t$  (for  $t = 1, \dots, T$ ) has a conditional multivariate normal distribution with parameters as derived below:

$$\begin{aligned}
& \Pr(\mathbf{d}_r | \mathbf{Y}) \propto \Pr(\mathbf{Y} | \mathbf{X}, \boldsymbol{\beta}, \mathbf{a}, \mathbf{d}_r, \mathbf{d}_{[-r]}, \mathbf{u}, \sigma_e^2) \times \Pr(\mathbf{d}_r) \\
& \propto \prod_{i>j} \exp \left\{ -\frac{1}{2\sigma_e^2} \|\mathbf{E}_{ij[-r]} - \mathbf{u}'_{ir} \mathbf{d}_r \mathbf{u}_{jr}\|^2 \right\} \times \exp \left\{ -\frac{1}{2} (\mathbf{d}'_r \mathbf{d}_r) \right\} \\
& \quad \text{where } \mathbf{E}_{ij[-r]} = \{E_{ij[-r]}^t\}_{t=1}^T \text{ (with } E_{ij[-r]}^t = E_{ij}^t + u_{ir}^t d_r^t u_{jr}^t \text{)} \text{ and } \mathbf{u}'_{ir} \mathbf{d}_r \mathbf{u}_{jr} = \{u_{ir}^t d_r^t u_{jr}^t\}_{t=1}^T \\
& \propto \exp \left\{ -\frac{1}{2\sigma_e^2} \left( \sum_{i>j} -2(\mathbf{E}_{ij[-r]} \mathbf{u}_{ir} \mathbf{u}_{jr})' \mathbf{d}_r + \mathbf{d}'_r (\text{diag}(\sum_{i>j} (\mathbf{u}_{ir} \mathbf{u}_{jr})^2)) \mathbf{d}_r \right) \right\} \times \exp \left\{ -\frac{1}{2} (\mathbf{d}'_r \mathbf{d}_r) \right\} \\
& \propto \exp \left\{ -\frac{1}{2} \left( \mathbf{d}'_r (I_T + \frac{\text{diag}(\sum_{i>j} (\mathbf{u}_{ir} \mathbf{u}_{jr})^2)}{\sigma_e^2}) \mathbf{d}_r - \frac{2}{\sigma_e^2} \left( \sum_{i>j} (\mathbf{E}_{ij[-r]} \mathbf{u}_{ir} \mathbf{u}_{jr})' \mathbf{d}_r \right) \right) \right\} \\
& \sim \mathcal{N}_T(\tilde{\boldsymbol{\mu}}_{\mathbf{d}_r}, \tilde{\boldsymbol{\Sigma}}_{\mathbf{d}_r}) \\
& \text{where } \tilde{\boldsymbol{\Sigma}}_{\mathbf{d}_r} = \left( I_T + \frac{\text{diag}(\{\sum_{i>j} (u_{ir}^t u_{jr}^t)^2\}_{t=1}^T)}{\sigma_e^2} \right)^{-1} \text{ and } \tilde{\boldsymbol{\mu}}_{\mathbf{d}_r} = \left( \frac{\{\sum_{i>j} (E_{ij[-r]}^t u_{ir}^t u_{jr}^t)\}_{t=1}^T}{\sigma_e^2} \right) \tilde{\boldsymbol{\Sigma}}_{\mathbf{d}_r}.
\end{aligned}$$

## B Metropolis-Hastings Algorithm for GP Parameters

For Gaussian process parameters—variance parameter  $\tau$  and length-scale parameter  $\kappa$ , we use the Metropolis-Hastings algorithm with a proposal density  $Q$  being the multivariate Gaussian distribution, with a diagonal covariance matrix—i.e.,  $\text{diag}(\sigma_{Q1}^2, \sigma_{Q2}^2)$ . Given the proposal variance  $\sigma_Q^2 = (\sigma_{Q1}^2, \sigma_{Q2}^2)$ , we sample the new values  $\tau'$  and  $\kappa'$  from

$$(\tau', \kappa') \sim \exp(\mathcal{N}_2(\log(\tau, \kappa), \sigma_Q^2 I_2)),$$

where we sample from the mean  $\log(\tau, \kappa)$  and exponentiate since both  $\tau$  and  $\kappa$  have to be positive. Under the symmetric proposal distribution as above, we accept the new proposed value  $(\tau', \kappa')$  with probability equal to

$$\min \left\{ 1, \frac{\Pr(\tau^{\eta'}, \kappa^{\eta'} | \boldsymbol{\eta}, k_\eta, \theta_\eta, \gamma)}{\Pr(\tau^\eta, \kappa^\eta | \boldsymbol{\eta}, k_\eta, \theta_\eta, \gamma)} \right\}$$

where  $\boldsymbol{\eta} = (\eta_1, \dots, \eta_T)$  can be any  $T$ -length vector of interest in our model (e.g.  $\boldsymbol{\beta}, \mathbf{a}, \mathbf{u}$ ).

Below are the acceptance ratios for all pairs of variables. In each case,  $\tau$  has a prior  $\tau \sim \mathcal{IG}(k_\eta, \theta_\eta)$ , and  $\kappa$  has a prior  $\kappa \sim \text{half-cauchy}(\gamma_\eta)$ .

1.  $(\tau_p^\beta, \kappa_p^\beta)$ , for  $p = 1, \dots, P$ :

$$\begin{aligned} \frac{\Pr(\tau_p^{\beta'}, \kappa_p^{\beta'} | \boldsymbol{\beta}_p, k_\beta, \theta_\beta, \gamma_\beta)}{\Pr(\tau_p^\beta, \kappa_p^\beta | \boldsymbol{\beta}_p, k_\beta, \theta_\beta, \gamma_\beta)} &= \frac{\Pr(\tau_p^{\beta'}, \kappa_p^{\beta'}, \boldsymbol{\beta}_p | k_\beta, \theta_\beta, \gamma_\beta)}{\Pr(\tau_p^\beta, \kappa_p^\beta, \boldsymbol{\beta}_p | k_\beta, \theta_\beta, \gamma_\beta)} \\ &= \frac{\Pr(\tau_p^{\beta'} | k_\beta, \theta_\beta) \Pr(\kappa_p^{\beta'} | \gamma_\beta) \Pr(\boldsymbol{\beta}_p | \tau_p^{\beta'}, \kappa_p^{\beta'})}{\Pr(\tau_p^\beta | k_\beta, \theta_\beta) \Pr(\kappa_p^\beta | \gamma_\beta) \Pr(\boldsymbol{\beta}_p | \tau_p^\beta, \kappa_p^\beta)}, \end{aligned}$$

where  $\boldsymbol{\beta}_p \sim \mathcal{N}_T(\mathbf{0}, \Sigma_p^\beta)$  with  $\Sigma_p^\beta = \tau_p^\beta f(\kappa_p^\beta)$ .

2.  $(\tau^a, \kappa^a)$

$$\begin{aligned} \frac{\Pr(\tau^{a'}, \kappa^{a'} | \mathbf{a}, k_a, \theta_a, \gamma_a)}{\Pr(\tau^a, \kappa^a | \mathbf{a}, k_a, \theta_a, \gamma_a)} &= \frac{\Pr(\tau^{a'}, \kappa^{a'}, \mathbf{a} | k_a, \theta_a, \gamma_a)}{\Pr(\tau^a, \kappa^a, \mathbf{a} | k_a, \theta_a, \gamma_a)} \\ &= \frac{\Pr(\tau^{a'} | k_a, \theta_a) \Pr(\kappa^{a'} | \gamma_a) \prod_{i=1}^N \Pr(\mathbf{a}_i | \tau^{a'}, \kappa^{a'})}{\Pr(\tau^a | k_a, \theta_a) \Pr(\kappa^a | \gamma_a) \prod_{i=1}^N \Pr(\mathbf{a}_i | \tau^a, \kappa^a)}, \end{aligned}$$

where  $\mathbf{a}_i \sim \mathcal{N}_T(\mathbf{0}, \Sigma^a)$  with  $\Sigma^a = \tau^a f(\kappa^a)$ .

3.  $(\tau_r^u, \kappa_r^u)$ , for  $r = 1, \dots, R$ :

$$\begin{aligned} \frac{\Pr(\tau_r^{u'}, \kappa_r^{u'} | \mathbf{u}_r, k_u, \theta_u, \gamma_u)}{\Pr(\tau_r^u, \kappa_r^u | \mathbf{u}_r, k_u, \theta_u, \gamma_u)} &= \frac{\Pr(\tau_r^{u'}, \kappa_r^{u'}, \mathbf{u}_r | k_u, \theta_u, \gamma_u)}{\Pr(\tau_r^u, \kappa_r^u, \mathbf{u}_r | k_u, \theta_u, \gamma_u)} \\ &= \frac{\Pr(\tau_r^{u'} | k_u, \theta_u) \Pr(\kappa_r^{u'} | \gamma_u) \prod_{i=1}^N \Pr(\mathbf{u}_{ir} | \tau_r^{u'}, \kappa_r^{u'})}{\Pr(\tau_r^u | k_u, \theta_u) \Pr(\kappa_r^u | \gamma_u) \prod_{i=1}^N \Pr(\mathbf{u}_{ir} | \tau_r^u, \kappa_r^u)}, \end{aligned}$$

where  $\mathbf{u}_{ir} \sim \mathcal{N}_T(\mathbf{0}, \Sigma_r^u)$  with  $\Sigma_r^u = \tau_r^u f(\kappa_r^u)$ .

## C List of Countries in Voting Network

Abbreviation	Country or area name	Abbreviation	Country or area name
AFG*	Afghanistan	KUW	Kuwait
ALB	Albania	LEB*	Lebanon
ALG	Algeria	LIB	Libya
ANG	Angola	MAA	Mauritania
ARG	Argentina	MEX	Mexico
AUL*	Australia	MLI	Mali
BAH	Bahrain	MOR	Morocco
BEN	Benin	MZM	Mozambique
BFO	Burkina Faso	NEW	New Zealand
BNG	Bangladesh	NIC	Nicaragua
BOL	Bolivia	NIG	Nigeria
BRA	Brazil	NIR	Niger
BUI	Burundi	NOR	Norway
BUL	Bulgaria	NTH	Netherlands
CAN	Canada	OMA	Oman
CAO	Cameroon	PAK*	Pakistan
CEN	Central African Republic	PAN	Panama
CHL	Chile	PAR	Paraguay
CHN*	China	PER	Peru
COL	Colombia	PHI	Philippines
CON	Congo	POL	Poland
COS	Costa Rica	POR	Portugal
DEN	Denmark	PRK*	North Korea
DOM	Dominican Republic	QAT	Qatar
ECU	Ecuador	ROK*	South Korea
EGY*	Egypt	RUS*	Russia
FIN	Finland	RWA	Rwanda
FRN*	France	SAL	El Salvador
GAB	Gabon	SAU	Saudi Arabia
GAM	Gambia	SEN	Senegal
GMV*	Germany	SIE	Sierra Leone
GHA	Ghana	SPN	Spain
GRC	Greece	SUD*	Sudan
GUA	Guatemala	SUR	Suriname
GUI	Guinea	SYR*	Syrian Arab Republic
GUY	Guyana	TAZ	Tanzania
HAI	Haiti	TOG	Togo
HON	Honduras	TRI	Trinidad and Tobago
HUN	Hungary	TUN	Tunisia
IND*	India	TUR*	Turkey
INS	Indonesia	UAE	United Arab Emirates
IRN*	Iran (Islamic Republic of)	UGA	Uganda
IRQ*	Iraq	UKG*	United Kingdom
ISR*	Israel	URU	Uruguay
ITA	Italy	USA*	United States of America
JAM	Jambia	VEN	Venezuela
JOR	Jordan	ZAM	Zambia
JPN*	Japan	ZIM	Zimbabwe
KEN	Kenya		

Table 2: Full list of the 97 countries, where the 21 most active countries during the ten year period of 2004 – 2014 (Hoff, 2015) are marked with \*.

## D Exploratory Summaries

Year	1983	1984	1985	1986	1987	1988	1989	1990	1991
Joint votes	126.709	128.302	134.563	139.387	133.998	123.612	104.472	78.943	61.753
Agreement	0.847	0.852	0.843	0.854	0.877	0.872	0.885	0.878	0.864
Year	1992	1993	1994	1995	1996	1997	1998	1999	2000
Joint votes	58.263	52.001	56.187	62.019	61.477	58.104	50.969	55.071	52.731
Agreement	0.842	0.835	0.847	0.835	0.844	0.831	0.851	0.837	0.839
Year	2001	2002	2003	2004	2005	2006	2007	2008	2009
Joint votes	50.362	58.282	63.418	61.860	59.651	73.235	64.857	62.353	57.893
Agreement	0.815	0.823	0.830	0.814	0.835	0.831	0.819	0.829	0.804
Year	2010	2011	2012	2013	2014				
Joint votes	57.336	54.404	60.216	56.016	66.197				
Agreement	0.822	0.798	0.823	0.802	0.814				

Table 3: Summary of the United Nations voting data for non-important votes: Average number of common votes (*upper*) and average voting similarity index (*lower*) per year.

Year	1983	1984	1985	1986	1987	1988	1989	1990	1991
Joint votes	7.384	7.441	8.129	9.201	8.283	5.121	12.605	7.361	8.559
Agreement	0.696	0.724	0.725	0.748	0.725	0.773	0.798	0.832	0.836
Year	1992	1993	1994	1995	1996	1997	1998	1999	2000
Joint votes	13.458	11.013	13.447	24.932	9.655	10.026	8.427	10.776	8.970
Agreement	0.806	0.773	0.785	0.827	0.765	0.805	0.776	0.829	0.768
Year	2001	2002	2003	2004	2005	2006	2007	2008	2009
Joint votes	9.191	12.826	12.142	8.432	8.855	10.956	10.681	10.845	10.946
Agreement	0.729	0.816	0.755	0.835	0.783	0.733	0.739	0.700	0.750
Year	2010	2011	2012	2013	2014				
Joint votes	12.289	9.067	7.575	10.171	12.048				
Agreement	0.744	0.751	0.733	0.754	0.847				

Table 4: Summary of the United Nations voting data for important votes: Average number of common votes (*upper*) and average voting similarity index (*lower*) per year.

correlation	log(distance)	polity	alliance	Trade/GDP	language
log(distance)	1.000	0.136	-0.508	-0.355	-0.286
polity	0.136	1.000	-0.264	-0.095	-0.142
alliance	-0.508	-0.264	1.000	0.275	0.417
Trade/GDP	-0.355	-0.095	0.275	1.000	0.100
language	-0.286	-0.142	0.417	0.100	1.000

Table 5: Pearson correlation coefficients between the observed dyadic covariates.

## E Posterior Predictive Checks on Degree Statistics

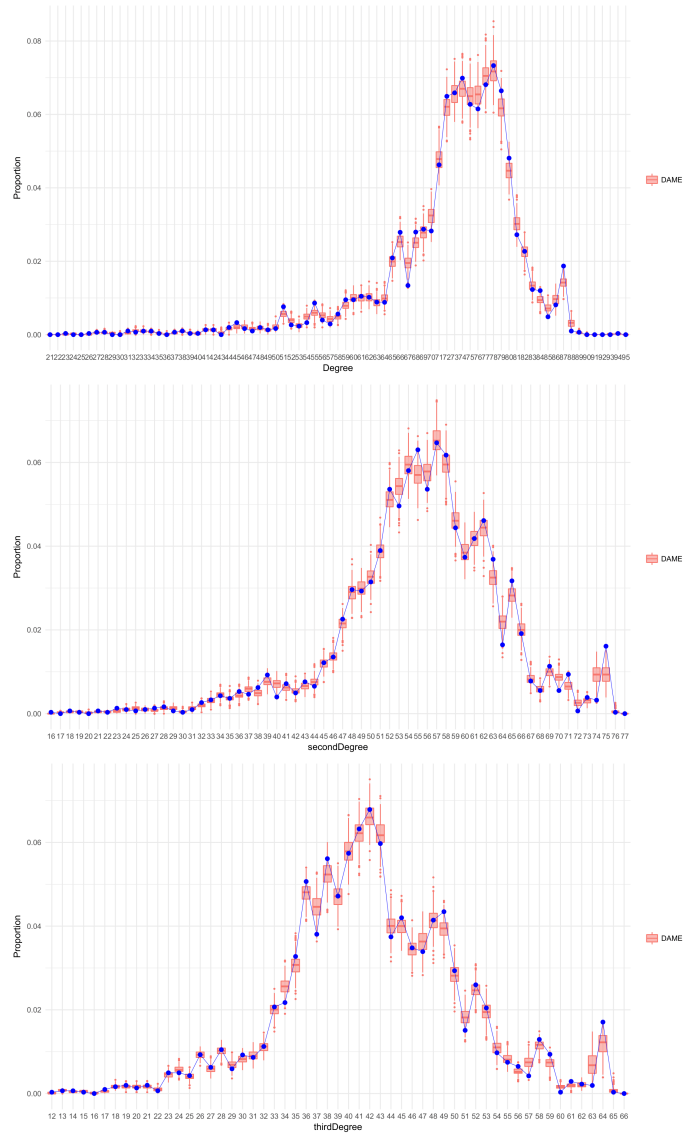


Figure 9: Posterior predictive plots of the overall degree distributions aggregating all nodes and timepoints: the first (*upper*), second (*middle*), and third moments (*lower*) shown with the dots representing observed statistics.